Published OnlineFirst February 11, 2013; DOI: 10.1158/0008-5472.CAN-12-2807

MDM2 Small-Molecule Antagonist RG7112 Activates p53 Signaling and Regresses Human Tumors in Preclinical Cancer Models

Christian Tovar, Bradford Graves, Kathryn Packman, Zoran Filipovic, Brian Higgins Mingxuan Xia, Christine Tardell, Rosario Garrido, Edmund Lee, Kenneth Kolinsky, Kwong-Him To, Michael Linn, Frank Podlaski, Peter Wovkulich, Binh Vu, and Lyubomir T. Vassilev

Abstract

MDM2 negatively regulates p53 stability and many human tumors overproduce MDM2 as a mechanism to restrict p53 function. Thus, inhibitors of p53-MDM2 binding that can reactivate p53 in cancer cells may offer an effective approach for cancer therapy. RG7112 is a potent and selective member of the nutlin family of MDM2 antagonists currently in phase I clinical studies. RG7112 binds MDM2 with high affinity ($K_D \sim 11$ nmol/L), blocking its interactions with p53 *in vitro*. A crystal structure of the RG7112–MDM2 complex revealed that the small molecule binds in the p53 pocket of MDM2, mimicking the interactions of critical p53 amino acid residues. Treatment of cancer cells expressing wild-type p53 with RG7112 activated the p53 pathway, leading to cell-cycle arrest and apoptosis. RG7112 showed potent antitumor activity against a panel of solid tumor cell lines. However, its apoptotic activity varied widely with the best response observed in osteosarcoma cells with *MDM2* gene amplification. Interestingly, inhibition of caspase activity did not change the kinetics of p53-induced cell death. Oral administration of RG7112 to human xenograft-bearing mice at nontoxic concentrations caused dose-dependent changes in proliferation/apoptosis biomarkers as well as tumor inhibition and regression. Notably, RG7112 was highly synergistic with androgen deprivation in LNCaP xenograft tumors. Our findings offer a preclinical proof-of-concept that RG7112 is effective in treatment of solid tumors expressing wild-type p53. *Cancer Res; 73(8); 2587–97. ©2013 AACR.*

Introduction

The tumor suppressor p53 plays a pivotal role in protection from cancer development. It is a transcription factor, which is activated following stress and regulates multiple downstream genes implicated in cell-cycle control, apoptosis, DNA repair, and senescence (1, 2). In nonstressed cells, the level of p53 is controlled by MDM2 through a negative feedback loop (3, 4). When nuclear p53 level is elevated, it activates the transcription of the *MDM2* gene. In turn, MDM2 protein binds to p53 and blocks its transactivation domain (5). MDM2 is also a p53-specific E3 ubiquitin ligase that targets p53 for ubiquitin-dependent degradation in the proteasome (6, 7). Both p53 and MDM2 have short half-lives and their nuclear concentrations are kept very low as a result of the functioning autoregulatory circuit (8, 9). However, in cancer cells overexpressing MDM2, this feedback loop is dysregulated (10). Stress-induced p53 activation mechanisms in these tumors are believed to be inadequate, leading to inefficient growth arrest and/or apoptosis (11). Therefore, blocking the p53-MDM2 interaction is expected to overcome the oncogenic consequences of MDM2 overproduction and to restore p53 function (12, 13).

Genetic and biochemical studies mapped p53-MDM2 binding sites to the N-terminal domain of MDM2 and the N-terminal part of the transactivation domain of p53 (5). The crystal structure of a p53-derived peptide bound to the p53-binding domain of MDM2 revealed the existence of a relatively deep cavity on the surface of the MDM2 molecule (14). More importantly, only 3 amino acid residues from the p53 peptide (Phe^{19}, Trp^{23}, and Leu^{26}) seemed to play a critical role in the binding between the 2 proteins by projecting residues deep into the hydrophobic cavity of the p53 pocket (14). These structural features of the p53–MDM2 complex suggested an increased likelihood of identifying small molecules that might interfere successfully with the protein–protein binding by mimicking the key amino acid contacts between the 2 proteins.

A class of imidazoline compounds has been identified as potent and selective inhibitors of the p53–MDM2 interaction (15). These molecules, termed nutlins, interact specifically with the p53-binding pocket of MDM2 and thus free p53 from negative control. Treatment of cancer cells expressing

Authors' Affiliation: Roche Research Center, Hoffmann-La Roche Inc., Nutley, New Jersey

Note: Supplementary data for this article are available at Cancer Research Online (http://cancerres.aacrjournals.org/).

C. Tovar, B. Graves, and K. Packman contributed equally to this work.

Corresponding Author: Lyubomir Vassilev, Discovery Oncology, Hoffmann-La Roche Inc., 340 Kingsland Street, Nutley, NJ 07110. Phone: 973-235-8106; Fax: 973-235-6185; E-mail: lubo.t.vassilev@gmail.com

doi: 10.1158/0008-5472.CAN-12-2807

Published OnlineFirst February 11, 2013; DOI: 10.1158/0008-5472.CAN-12-2807

wild-type p53 with nutlins stabilizes p53 and activates the p53 pathway leading to activation of p53 target genes, cell-cycle arrest, and apoptosis (16). Although nutlins have shown good cellular activity and allowed to derive the mechanistic proof-of-concept for targeting p53–MDM2 interaction for cancer therapy, their pharmacologic properties were inadequate for clinical development. Here, we describe a potent and selective new member of the nutlin family of MDM2 antagonists, RG7112, which has been optimized for clinical use. It binds selectively to the p53 pocket on the surface of the MDM2 *in vitro* with high affinity, blocks p53–MDM2 binding, leading to stabilization and accumulation of p53 protein and activation of the p53 pathway. The compound has good oral bioavailability and has shown strong tumor growth inhibition and regression in mouse xenograft models of human cancer supporting its development for cancer therapy.

Materials and Methods

Cells, reagents, and assays

Cell lines were maintained in the recommended media supplemented with 10% heat-inactivated FBS (Invitrogen) and 2 mmol/L L-glutamine (Invitrogen). For some cell lines, modifications were made to standard growth media. MDA-MB-435 cells were maintained in media supplemented with 1 mmol/L sodium pyruvate. Unless otherwise indicated, all media were supplied by Invitrogen. MDA-MB-435 cells were provided by Dr. Patricia Steeg from the National Cancer Institute (Bethesda, MD) upon permission of Dr. Janet Price (MD Anderson Cancer Center, University of Texas, Houston, TX). The 22Rv1 cell line was kindly provided by Dr. James W. Jacobberger (Case Western University, Cleveland, OH). MHM cells were derived from an osteosarcoma with amplified *MDM2* gene and kindly provided by Dr. Ola Myklebost (Radium Hospital, Oslo, Norway). All other cell lines were obtained from the American Type Culture Collection.

Recombinant human GST-MDM2 was cloned, expressed, and purified at Roche. Phycolink goat anti-GST (type 1) allophycocyanin was purchased from Prozyme and Eu-8044-streptavidin was purchased from Perkin Elmer. Biotinylated MDM2 substrate peptide (Biotin-Aca-Met-Pro-Arg-Phe-Met-Asp-Tyr-Trp-Glu-Gly-Leu-Asn-NH2) was synthesized at Roche using standard methods. All chemicals were purchased from Sigma unless indicated otherwise.

The test compound [(4S,5R)-2-(4-tert-Butyl-2-ethoxy-phenyl)-4,5-bis-(4-chloro-phenyl)-4,5-dimethyl-4,5-dihydro-imidazol-1-yl]-[4-(3-methanesulfonyl-propyl)-piperazin-1-yl]-methanone was synthesized at Hoffmann-La Roche. To prepare stock solutions, compounds were dissolved at 10 mmol/L in 100% dimethyl sulfoxide (DMSO) and stored at −20°C.

Homogeneous time-resolved fluorescence (HTRF) assay measures the signal generated by 2 components when they are in close proximity. The p53–MDM2 binding assay uses a biotinylated peptide derived from the MDM2-binding domain of p53 and a truncated N-terminal portion of recombinant human GST-tagged MDM2 protein containing the p53-binding domain. Proteins for crystal structure studies were expressed in *E. coli* strain BL21 using the helper plasmid pUBS 520 coding for the $lacI^q$ repressor and the rare $tRNA^{Arg}$ [AGA/AGG]. For crystallization, the frozen protein was thawed and concentrated to 9.8 mg/mL using a Centricon concentrator (3,000 MW cutoff). The complex was then formed by combining the protein with a slight molar excess of the inhibitor (stock solution is 100 mmol/L in DMSO) and this solution was allowed to sit for 4 hours at 4°C. Cryopreserved crystals were used to collect diffraction data on beamline X8C at the National Synchrotron Light Source at Brookhaven National Laboratory (Upton, NY).

Cell proliferation/viability was evaluated by the tetrazolium dye (MTT) assay. Cell growth kinetics were measured using the IncuCyte live cell imaging system (Essen BioScience, Inc.). For cell-cycle analysis, cells were cultured in T75 flask with appropriate growth medium (10^6 cells/condition in 10 mL) and incubated overnight at 37°C. They were incubated with test compounds and processed as previously described (16). Apoptosis was determined using the Annexin V assay using the GuavaNexin apoptosis detection kit (Guava Technologies) and percent apoptosis determined by using a Guava Personal Cell Analyzer following the manufacturer's protocol.

Animal studies

For SJSA-1, SJSA-1luc2, and MHM xenograft studies, female Balb/c nude (CAnN.Cg-*Foxn1nu*/Crl, Charles River Laboratories; Wilmington, DE) mice were implanted subcutaneously in the right flank with 5×10^6 cells suspended in a 0.2 mL volume of a 1:1 mixture of Matrigel:PBS. For studies with hormone-dependent LNCaP xenografts, castrated male Balb/c nude (CAnN.Cg-*Foxn1nu*/Crl, Charles River Laboratories) were implanted with 12.5 mg sustained-release testosterone pellets (Innovative Research of America) 5 days before subcutaneous inoculation with 1×10^7 cells suspended in 0.2 mL of Matrigel:PBS. Mice were randomized into treatment groups ($n = 10$ per group) when mean tumor volume reached approximately 150 to 400 mm^3. In all studies, mice received either vehicle (1% Klucel LF/0.1% Tween 80) or RG7112, administered as an oral suspension at the dose indicated (25–200 mg/kg). For assessment of androgen ablation treatment in combination with RG7112 in LNCaP xenograft-bearing mice, testosterone pellets were removed under ketamine/xylazine anesthesia. Tumor volume was monitored by caliper measurement and body weights were recorded 2 to 3 times weekly. Tumor volume (in mm^3) was calculated as described previously (17).

For Western blot analysis, mice bearing established SJSA-1 subcutaneous xenografts received a single oral dose of vehicle or 50, 100, or 200 mg/kg RG7112, and tumors were harvested at 4 and 8 hours after dosing. Protein was extracted from tumor tissue with 1× radioimmunoprecipitation assay buffer (Sigma Aldrich) containing protease inhibitors (Roche Diagnostics) by homogenization. Equal amounts of total protein were resolved on 4% to 12% NuPAGE gradient gel (Invitrogen) and blotted with antibody dilutions as recommended by manufacturer. The chemiluminescent signal was generated with enhanced chemiluminescence Plus (GE Healthcare) and detected with Fujifilm LAS-3000 imager. The densitometric quantitation of specific bands was determined using Multi Gauge Software

Published OnlineFirst February 11, 2013; DOI: 10.1158/0008-5472.CAN-12-2807

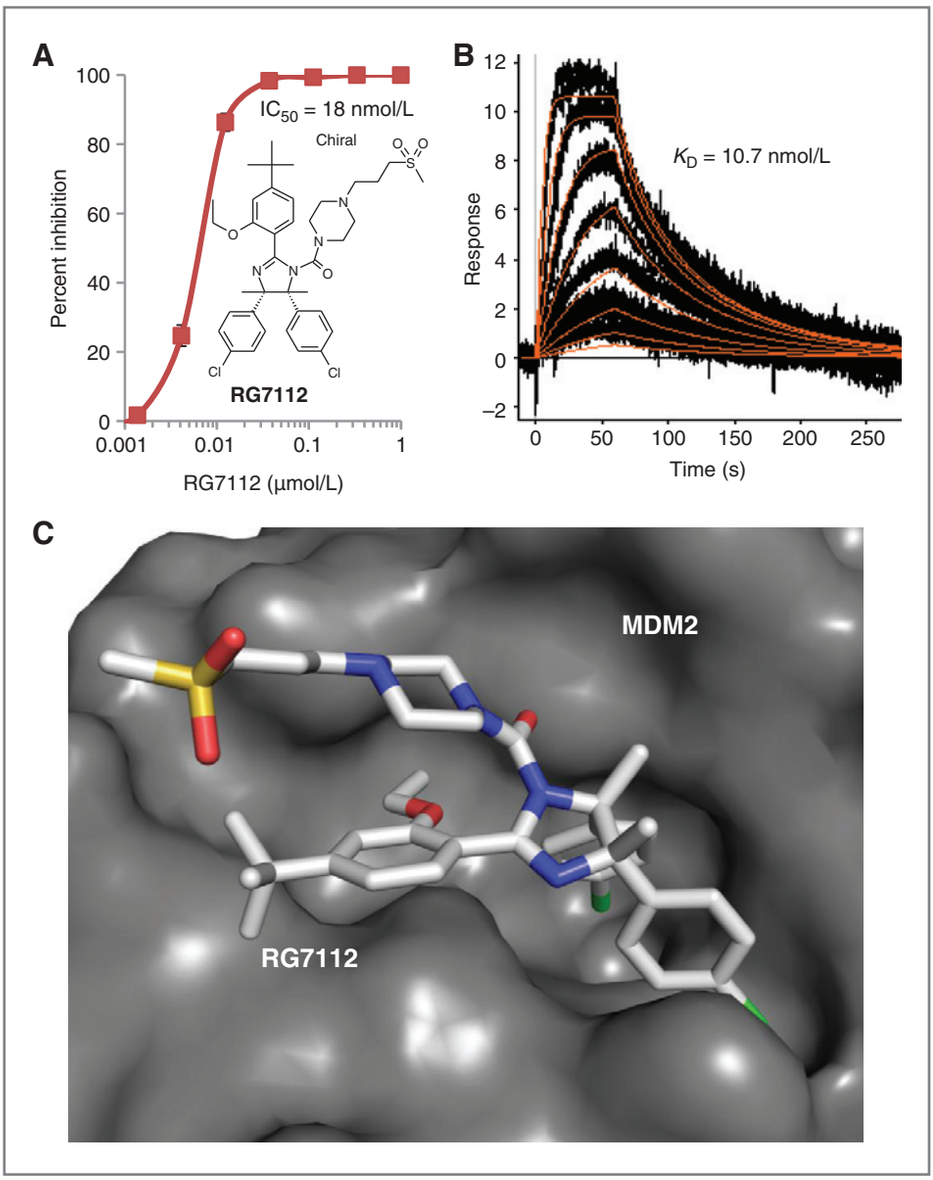

Figure 1. *In vitro* binding properties of RG7112. A, chemical structure and *in vitro* activity of RG7112. Inhibitory effect of RG7112 on p53-MDM2 binding was measured by the HTRF assay and expressed as concentration, causing 50% inhibition (IC_{50}). B, RG7112 binds MDM2 with high affinity. Direct binding of RG7112 was determined with the Biacore instrument by measuring response rates at a variety of concentrations. C, crystal structure of RG7112 bound to MDM2. The surface of MDM2 is shown in gray and the stick figure of RG7112 is colored according to element type: white for carbon atoms, blue for nitrogen atoms, red for oxygen atoms, yellow for the sulfur atom, and green for the chlorine atoms. The MDM2 antagonist sits in the p53 binding pocket and the 3 key residue binding sites normally occupied by Phe^{19}, Trp^{23}, and Leu^{26} from p53 are instead occupied by the ethoxy group and the 2 chloro-phenyl groups, respectively.

(Fujifilm). The complete methods can be found in the online Supplementary Information.

Results

RG7112 is a potent inhibitor of p53-MDM2 binding

Nutlins (15) represented the starting point for a lead optimization effort that culminated in the selection of RG7112 as a clinical lead. This compound is a more potent binder to MDM2 than the original nutlins (15, 16). In the cell-free p53-MDM2 binding assay, RG7112 was able to displace a p53 peptide from the surface of MDM2 with an IC_{50} of 18 ± 11 nmol/L (Fig. 1A). This is approximately 4-fold higher potency than nutlin-3a (15). Consistent with previous findings for nutlin-3 (15), the inactive enantiomer of RG7112 was approximately 200-fold less potent in the binding assay (data not shown). Supporting the results from the p53-MDM2 binding assay, Biacore experiments showed that RG7112 binds to MDM2 with an equilibrium K_D of 10.7 nmol/L (Fig. 1B). This improvement in binding as compared with nutlin-3a results from the combined effect of a faster on-rate and a slower off-rate (Supplementary Fig. S1).

Published OnlineFirst February 11, 2013; DOI: 10.1158/0008-5472.CAN-12-2807

Similarly to nutlin-3a, RG7112 is a specific MDM2 inhibitor and practically inactive against MDMX (data not shown). In addition to the enhanced binding properties, RG7112 exhibited significant improvements in pharmacologic properties. The 4,5-dimethyl substitution (Fig. 1A) imparts greater structural rigidity to the imidazoline scaffold and blocks metabolic conversion to the inactive imidazole form (manuscript in preparation).

A crystal structure of RG7112 with MDM2 (Fig. 1C) revealed that the small molecule binds in the same fashion to the p53 pocket as was first described for nutlin-2 (15). The 2 chlorophenyl rings occupy the Trp^{23} and Leu^{26} pockets, whereas the ethoxy group projects into the Phe^{19} pocket. An overlay of the RG7112 structure with that of nutlin-2 (Supplementary Fig. S2) shows that the dimethyl substitution has not distorted the imidazoline ring in any significant way. This is consistent with the observation that the additional rigidity has not sacrificed binding.

RG7112 stabilizes wild-type p53 and induces p53 signaling in cancer cells

Treatment of cultured cancer cells with RG7112 led to concentration-dependent accumulation of p53 protein and its transcriptional targets, p21 and MDM2 (Fig. 2A). These changes were due to transcriptional activation as revealed by the dose-dependent induction of their mRNA as well as that of another p53 transcriptional target, MIC-1 (ref 18; Fig. 2B) and reflect the inability of MDM2 ligase to bind to and target p53 for ubiquitin-dependent degradation as previously shown for nutlin (15, 16). Under the same conditions, the inactive

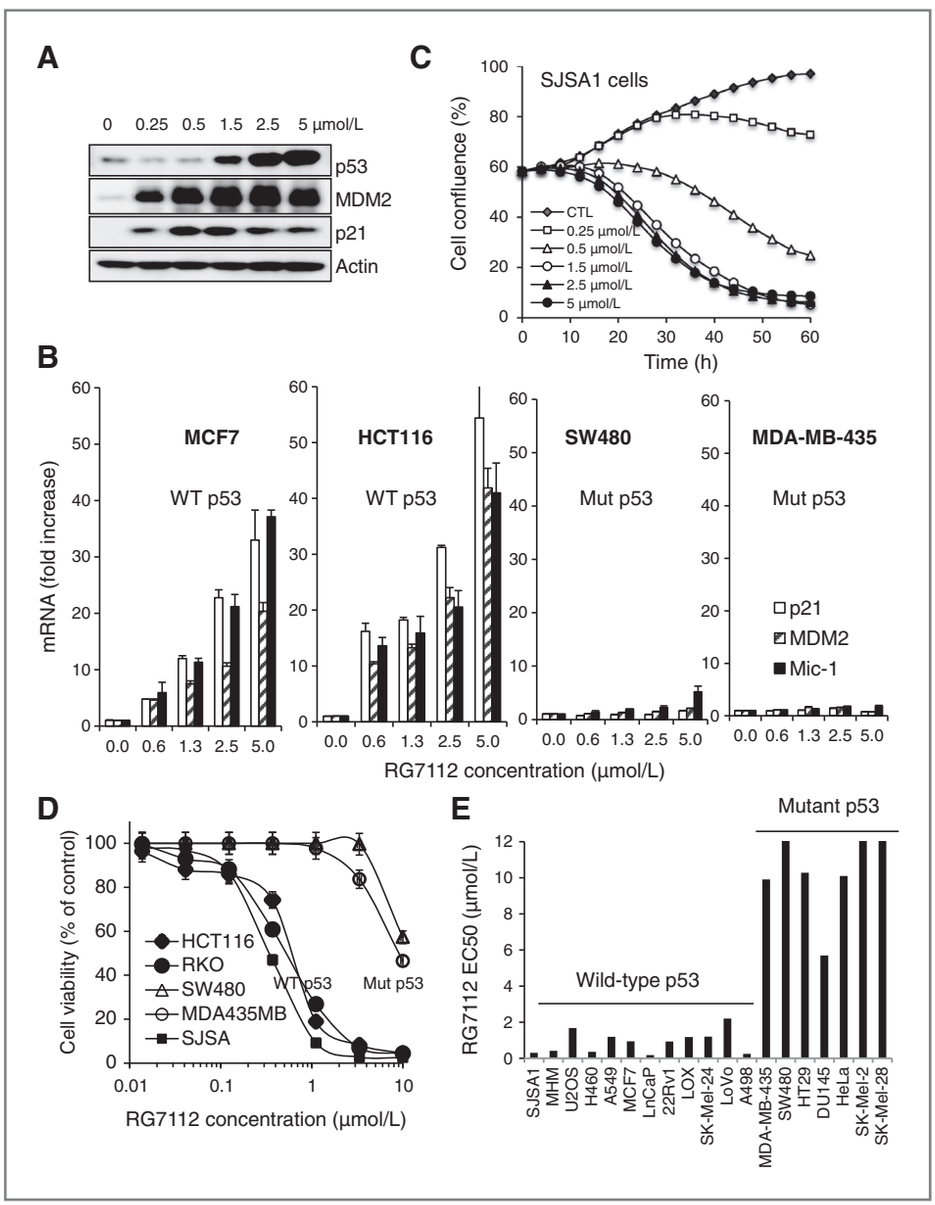

Figure 2. RG7112 activates p53 signaling in cancer cells expressing wild-type p53. A, RG7112 dose dependently accumulates p53 protein and its targets, MDM2 and p21 in SJSA1 osteosarcoma cells. Protein levels were analyzed by Western blotting 24 hours after addition of RG7112 to exponentially growing cells. B, RG7112 activates p53 target genes in cells with wild-type but not mutant p53. Two cancer cell lines expressing wild-type p53 (MCF7 and HCT116) and 2 mutant p53 lines (SW480 and MDA-MB-435) were incubated with increasing RG7112 concentrations for 24 hours and the mRNA of 3 p53-target genes (p21, MDM2, and MIC-1) were determined by quantitative PCR and expressed as fold-change from DMSO controls. C, RG7112 inhibits the growth and kills SJSA1 osteosarcoma cells in a dose-dependent manner. Exponentially growing cells were incubated with indicated concentration of RG7112 or DMSO vehicle and kinetics of cell growth was measured by continuous time-lapse cell imaging using the IncuCyte instrument. D, RG7112 cytotoxicity depends on the p53 status of cancer cells. Three wild-type p53 (HCT116, RKO, and SJSA1) and 2 mutant p53 (SW480 and MDA-MB-435) exponentially growing cancer cell lines were incubated with RG7112 for 5 days and cell viability was measured by the MTT assay. E, cancer cells expressing wild-type p53 are more sensitive to cytotoxic effect of RG7112. RG7112 activity was tested on a panel of 19 cancer cells lines as in D.

Published OnlineFirst February 11, 2013; DOI: 10.1158/0008-5472.CAN-12-2807

enantiomer of RG7112 does not affect cellular p53 level (data not shown). Activation of p53 was not due to genotoxic mechanism induced by RG7112, as no change in the phosphorylation status of Ser^{15} on p53 protein was detected upon treatment of cancer cells with 10 μmol/L RG7112 for 24 hours (Supplementary Fig S3). No changes in the mRNA levels of all 3 p53 targets were detected in cancer cells expressing mutant p53, which is unable to bind DNA and therefore inactive as a transcription factor (Fig. 2B).

RG7112 dose dependently inhibited the growth and killed SJSA1 osteosarcoma cells expressing high-levels of MDM2 protein due to *MDM2* gene amplification (Fig. 2C). The onset of cell death was relatively slow with visual signs of adhesion loss 15 to 20 hours after addition of RG7112 at concentrations greater than 1 μmol/L. As expected from the mechanism of action, growth suppressive and cytotoxic effect of RG7112 was clearly dependent on the p53 status of cancer cells. In the 5 cell line panel (3 wild-type and 2 mutant p53 lines) used routinely for screening, there was more than 10-fold difference in sensitivity (Fig. 2D). This difference was confirmed when RG7112 was tested on an additional 12 wild-type and 7 mutant p53 cell lines (Fig. 2E). RG7112 inhibited the proliferation of 15 of 15 cancer cell lines expressing wild-type p53 (IC_{50} range: 0.18–2.2 μmol/L), but to a much lesser extent inhibited 7 cancer cell lines with p53 mutation (EC_{50} range: 5.7–20.3 μmol/L; Supplementary Table S1). The overall selectivity between the panels of 7 mutant and 15 wild-type p53 lines, expressed as fold difference in the average IC_{50} values, was 14-fold. RG7112 showed similar margin of selectivity between the HCT116 cancer cell line and its p53-null clone HCT115R1 (Supplementary Fig. S4).

RG7112 effectively activates p53 functions in cancer cells

Cell-cycle arrest is one of the main cellular functions of activated p53. The tumor suppressor effectively arrests cell-cycle progression in G_1 and G_2 phases primarily attributed to induction of the p53 transcriptional target and pan-cyclin–dependent kinase inhibitor, p21 (19, 20). Treatment of exponentially proliferating cancer cells (HCT116 and SJSA1) with RG7112 for 24 hours induced a dose-dependent cell-cycle block in G_1 and G_2–M phase and depletion of the S-phase compartment (Fig. 3A). In the MDM2-overexpressing osteosarcoma cell line, SJSA1, the cell-cycle arrest was followed by induction of apoptosis as revealed by the Annexin V assay (Fig. 3B). As shown previously with nutlin-3a, (16) the cell-cycle arrest function was activated in all tested solid tumor cell lines of epithelial origin (data not shown) but its apoptotic activity varied widely in the 12 cancer cell line panels (Fig. 3C). The 2 osteosarcoma cell lines with *MDM2* gene amplification exhibited the highest sensitivity and the majority of the cell population underwent apoptotic cell death. The sensitivity of the rest ranged from very good (LNcaP) to poor (U2OS). Practically, half of the cell lines in the panel were unable to undergo apoptosis in the presence of high RG7112 concentration, similar to results with nutlin-3a (16). As previously shown (16, 21), this resistance to apoptotic activity of the MDM2 antagonists was not due to inability to stabilize p53 or induce its target genes.

Although both cell-cycle arrest and apoptotic function of p53 depend on its transcriptional activity, they are executed via different downstream pathways and may require different threshold levels of p53 protein. To test this hypothesis, we determined the RG7112 concentration required for achieving 50% of the maximum cell-cycle arrest or apoptosis in the sensitive osteosarcoma cell line, SJSA1. To this end, we used a range of drug concentrations allowing to reach less than 1% S-phase fraction for cell-cycle arrest after 24 hours or a plateau effect for Annexin V positivity after 48 hours incubation with RG7112. EC_{50} for cell-cycle arrest (0.4 μmol/L) was found to be lower than EC_{50} for apoptosis (1 μmol/L) by 2.5-fold (Fig. 3D).

Caspase inhibition does not affect the onset of RG7112-induced cell death

Caspase deficiency is a frequent event in cancer and may affect tumor response to apoptosis-inducing therapies including MDM2 antagonists. Therefore, we asked how the loss of caspase activity would affect the response to RG7112. To this end, we used a highly sensitive cancer cell line, SJSA1, and RG7112 concentration capable of inducing robust apoptosis in the presence or absence of the potent pan-caspase inhibitor, Z-VAD-FMK. After 48-hour incubation, RG7112 induced high levels of Annexin V indicative of massive cell death that was reduced substantially by pretreatment with Z-VAD (Fig. 4A). However, cell death kinetics measured by the percentage of viable cells remained unchanged (Fig. 4B). The levels of p53 and its targets, p21 and MDM2, were also similar in the presence or absence of caspase inhibitor (Fig. 4C). Then, we followed cell morphology over several days in the presence or absence of Z-VAD-FMK. RG7112 treatment caused clear apoptotic phenotype with nuclear fragmentation and chromatin condensation after 48 hours (Fig. 4D, left). However, in the presence of caspase inhibitor, the dead SJSA1 cells preserved their intact nuclear morphology for several days (Fig. 4D, right). Thus, caspase inhibition turned RG7112-induced apoptotic death into a necrotic-like death. This phenomenon was not limited to RG7112 but was also observed with nutlin-3a (data not shown) suggesting that MDM2 antagonists do not require caspase activity for effective cell killing.

RG7112 activates p53 pathway and induces apoptosis in tumor cells *in vivo*

Pharmocodynamic effects of RG7112 were assessed in the SJSA1 xenograft model. Disruption of p53-MDM2 binding by RG7112 led to stabilization of p53, activation of the pathway, and elevation of p53 target genes such as p21 and MDM2 *in vitro* (Fig. 2). To assess the ability of RG7112 to activate p53 response *in vivo*, SJSA1 tumor-bearing mice were treated with a single dose of vehicle or 50 to 200 mg/kg RG7112 for 4 to 24 hours (Fig. 5A). Western blot analysis showed a dose-dependent increase in p53 protein and its targets, p21 and MDM2. The p53 protein levels were highest at 4 hours after dose and continue to persist at 24 hours at the highest dose level (200 mg/kg), whereas the duration of p53 modulation was shorter at lower dose levels.

Activation of p53 in SJSA1 cells showed effective cell-cycle arrest, followed by apoptosis *in vitro* (Fig. 3). *In vivo*, we

Published OnlineFirst February 11, 2013; DOI: 10.1158/0008-5472.CAN-12-2807

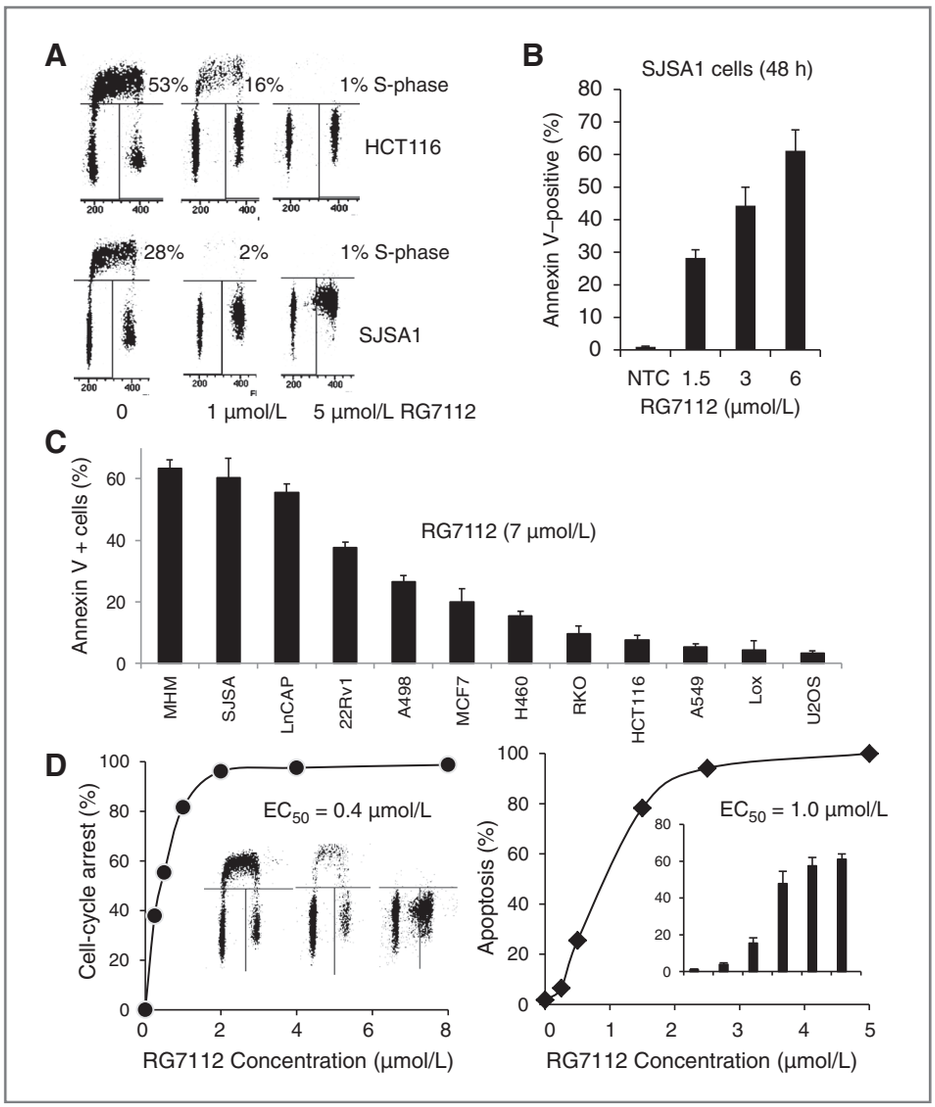

Figure 3. RG7112 induces cell-cycle arrest and apoptosis in cancer cells. A, RG7112 arrests cancer cells with wild-type p53 in G_1 and G_2 phases. Log-phase cancer cells were incubated with RG7112 or DMSO for 24 hours and their cell-cycle distribution was determined by BrdUrd labeling and cell-cycle analysis. B, RG7112 induces apoptosis in osteosarcoma cells with *mdm2* gene amplification. Exponentially proliferating cells were exposed to RG7112 for 48 hours and the fraction of Annexin-positive cells was determined by the Nexin assay. C, apoptotic activity of RG7112 varies among solid tumor cells. A panel of 11 solid tumor derived cancer cell lines were incubated with 7 μmol/L RG7112 for 48 hours and apoptotic activity was measured by the Annexin V assay. D, lower RG7112 levels are required for cell-cycle arrest versus apoptosis. Exponentially growing SJSA1 osteosarcoma cells were incubated with a range of RG7112 concentrations and the IC_{50} for reaching maximum cell-cycle inhibition (depletion of S-phase compartment) and apoptosis (Annexin V positivity) were determined as in A and B.

assessed cell-cycle arrest by measuring bromodeoxyuridine (BrdUrd) incorporation. SJSA1 tumor-bearing animals were treated with a single dose of vehicle or 50 to 200 mg/kg RG7112 for 8 to 24 hours, and BrdUrd was administered 2 hours before tumor collection. Immunohistochemical detection of BrdUrd incorporation indicated a statistically significant and dose-dependent decrease in proliferating cells at 16 and 24 hours postdosing with RG7112 as compared with vehicle controls (Fig. 5B.). At the highest dose level of RG7112 (200 mg/kg), only 1.2% (± 0.89 SD) of cells incorporated BrdUrd at 24 hours postdosing versus 14% (± 1.83 SD) of vehicle treated tumors, suggesting that RG7112 effectively arrests DNA replication and tumor cell proliferation.

p53-Dependent apoptosis typically involves proteolytic activation of caspase-3 and 7, which in turn cleave substrates containing a short DEVD amino acid sequence. Presence of activated caspases 3 and 7 are viewed as "early" markers of apoptosis, as they can be detected before plasma membrane blebbing and DNA fragmentation. To evaluate the ability of RG7112 to elicit apoptosis *in vivo*, bioluminescent detection of activated caspases 3/7 was monitored in SJSA1-luc2 tumor-bearing mice using Z-DEVD-aminoluciferin as a substrate for activated caspases 3 and 7. When the DEVD peptide sequence is cleaved by activated caspases, aminoluciferin is liberated and can then serve as a substrate for luciferase enzyme produced by SJSA1-luc2 cells. Luminescent signal is thereby emitted only in apoptotic cells. Representative bioluminescent images from mice bearing vehicle and RG7112-treated tumors are shown in Fig. 5C (left). Tumors from mice treated with a single dose of 100 or 200 mg/kg RG7112 produced a statistically significant time-dependent induction in luciferase signal as compared with vehicle controls, indicating that apoptosis was occurring within the tumors (Fig. 5C, right).

PARP is a caspase-3 substrate whose cleavage product is observed during apoptotic cell death (cPARP). Immunohistochemical detection of cPARP was conducted in SJSA1

Published OnlineFirst February 11, 2013; DOI: 10.1158/0008-5472.CAN-12-2807

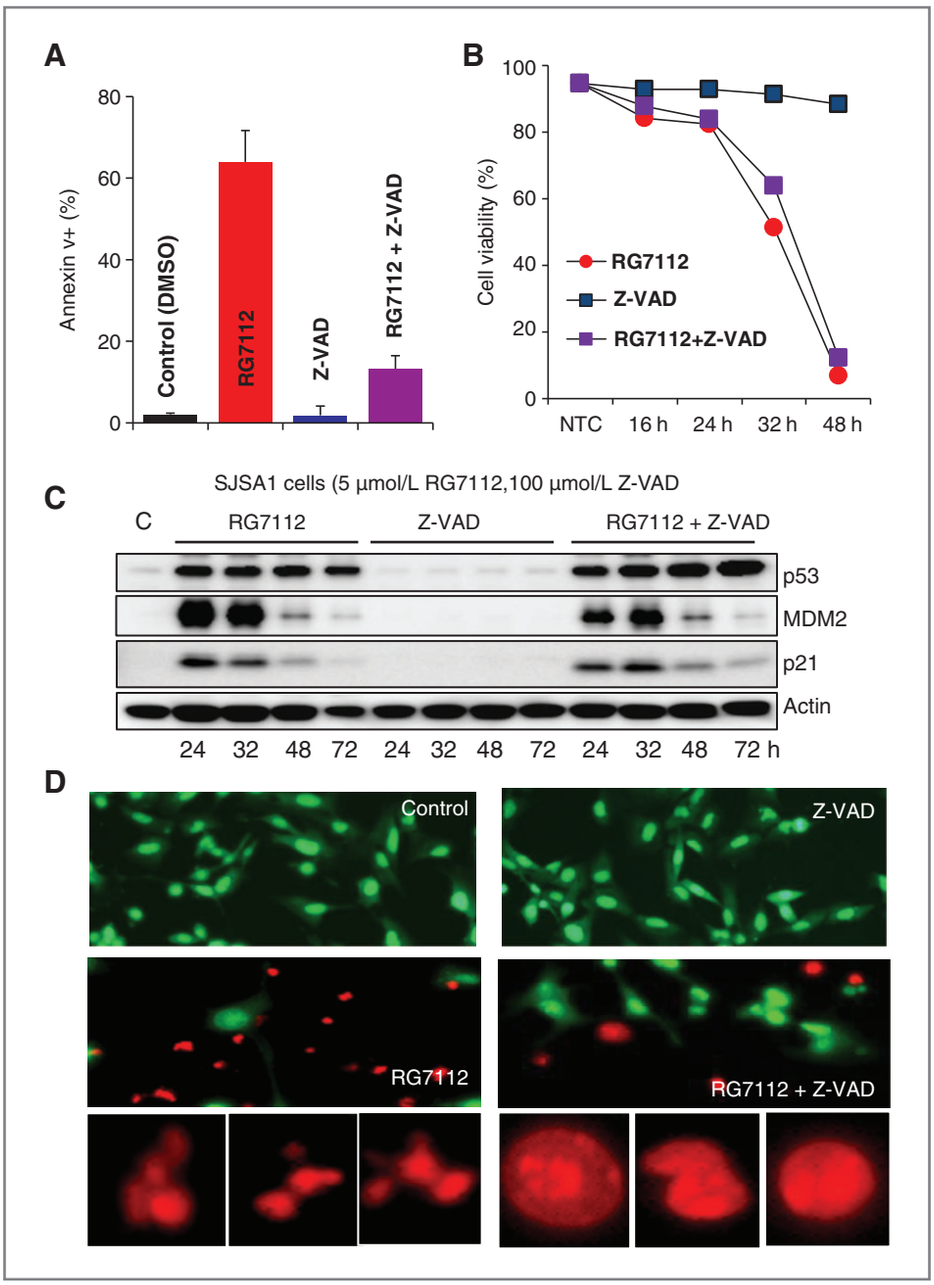

Figure 4. Inhbition of caspase activity does not affect the kinetics of cell death induced by RG7112. A, caspase inhibition reduces RG7112-induced Annexin V–positive cells. SJSA1 osteosarcoma cells were incubated with 7 μmol/L RG7112 in the presence or absence of 100 μmol/L Z-VAD-FMK for 48 hours and Annexin V–positive cell fraction was determined by the Guava Nexin assay. B, caspase inhibition does not affect the kinetics of RG7112-induced cell death. SJSA1 cells were incubated with 5 μmol/L RG7112 in the presence or absence of 100 μmol/L Z-VAD-FMK for 48 hours and cell viability was determined at indicated times and plotted as percent of untreated controls. C, RG7112-induced changes in p53, p21, and MDM2 in the presence of Z-VAD-FMK by Western blotting. D, caspase inhibition changes morphologic signs of cell death by RG7112. SJSA1 cells were incubated with RG7112 ± Z-VAD-FMK as above for 6 days and cell morphology was examined by fluorescence microscopy after staining with acridine orange/propidium iodide.

xenografts at various time points (8–24 hours) postdosing with a single dose of vehicle or 50 to 200 mg/kg RG7112 (Fig. 5D). A statistically significant increase in cPARP was detected in tumors 16 and 24 hours postdosing with 200 mg/kg RG7112, whereas lower doses were similar to vehicle-treated controls (Fig. 5D, right). Cells staining positively for cParp exhibited typical apoptotic morphology such as condensation and nuclear fragmentation (Fig. 5D, left).

The observed pharmacodymanic effects in SJSA-1 xenografts treated with a single dose of RG7112 confirmed that the drug can penetrate tumor cells *in vivo* and can activate p53 and its 2 major functions, cell-cycle arrest and apoptosis. RG7112 blocked the proliferation of exponentially growing mouse NIH-3T3 fibroblasts, suggesting that it effectively inhibits mouse MDM2 protein and activates cell-cycle arrest function of p53 in mouse cells (Supplementary Fig. S5).

RG7112 regresses human xenografts in nude mice

We tested the antitumor activity of MDM2 inhibitor in 2 models of human osteosarcoma with *MDM2* gene amplification and overexpression of MDM2 protein, SJSA1 and MHM. Daily oral administration of RG7112 inhibited both human osteosarcoma xenografts in a dose-dependent manner with 74% and 69% tumor growth inhibition elicited, respectively, at

Published OnlineFirst February 11, 2013; DOI: 10.1158/0008-5472.CAN-12-2807

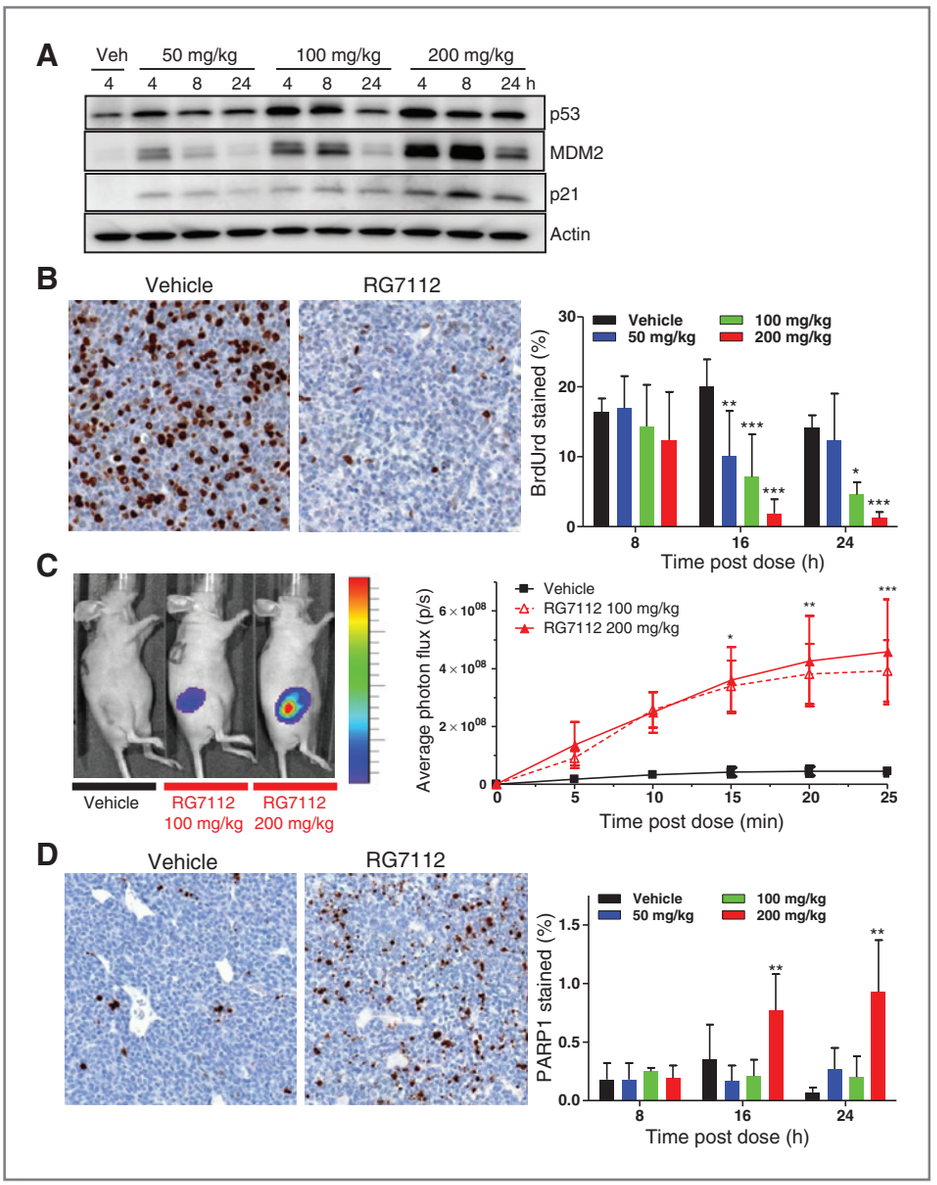

Figure 5. Pharmacodynamics of RG7112 in SJSA1-bearing nude mice. A, Western blot analysis of changes in p53, MDM2, and p21 expression in SJSA1 xenografts. Lysates were prepared from tumors treated with vehicle or 50, 100, or 200 mg/kg RG7112 ($n = 3$/group). B, immunohistochemical detection of BrdUrd incorporation. Animals were given a single dose of vehicle or 50 to 200 mg/kg RG7112 and pulsed with BrdUrd 2 hours before sample collection ($n = 5$/group). Left, representative micrographs of BrdUrd staining 24 hours postvehicle or RG7112 administration. Right, quantitation of BrdUrd incorporation at multiple time points and RG7112 concentrations. Data was plotted as mean ± SD. *, $P < 0.05$; **, $P < 0.01$, ***, $P < 0.001$ versus vehicle control. C, bioluminescent imaging of activated caspase and caspase 7 in tumor-bearing mice treated with RG7112. Mice ($n = 5$/group) bearing subcutaneous SJSA-1 xenografts received a single 200 mg/kg dose of RG7112 or vehicle. At indicated times postdosing, mice were given 50 mg/kg zDEVD-aminoluciferin i.v. and images were captured 20 minutes later (left). In each treatment group, bioluminescent imaging was conducted from 5 to 25 minutes post-zDEVD-aminoluciferin administration (right). Data plotted as mean ± SEM. *, $P < 0.05$, **, $P < 0.01$, ***, $P < 0.001$ versus vehicle control. D, immunohistochemical detection of cleaved PARP-1. Animals were given a single dose of vehicle or 50 to 200 mg/kg RG7112. Left, representative micrographs of cleaved PARP-1 staining 24 hours after vehicle or RG7112 administration. Right, quantitation of cleaved PARP-1 staining at multiple time points and RG7112 concentrations. Data was plotted as mean ± SD. *, $P < 0.05$, **, $P < 0.01$, ***, $P < 0.001$ versus vehicle control.

a daily dose of 50 mg/kg (Fig. 6A and B). At the high dose of 100 mg/kg, the majority of SJSA1 and MHM tumors regressed and the average tumor volume was below the starting volume.

We have shown previously that MDM2 antagonists can synergize with androgen ablation in the androgen-dependent prostate cancer cell line LNCaP (17). RG7112 was tested in the LNCaP androgen deprivation model (Fig. 6). Although daily administration of 100 mg/kg RG7112 or androgen withdrawal effectively inhibited tumor growth and induced partial tumor regression, their combination caused a

Published OnlineFirst February 11, 2013; DOI: 10.1158/0008-5472.CAN-12-2807

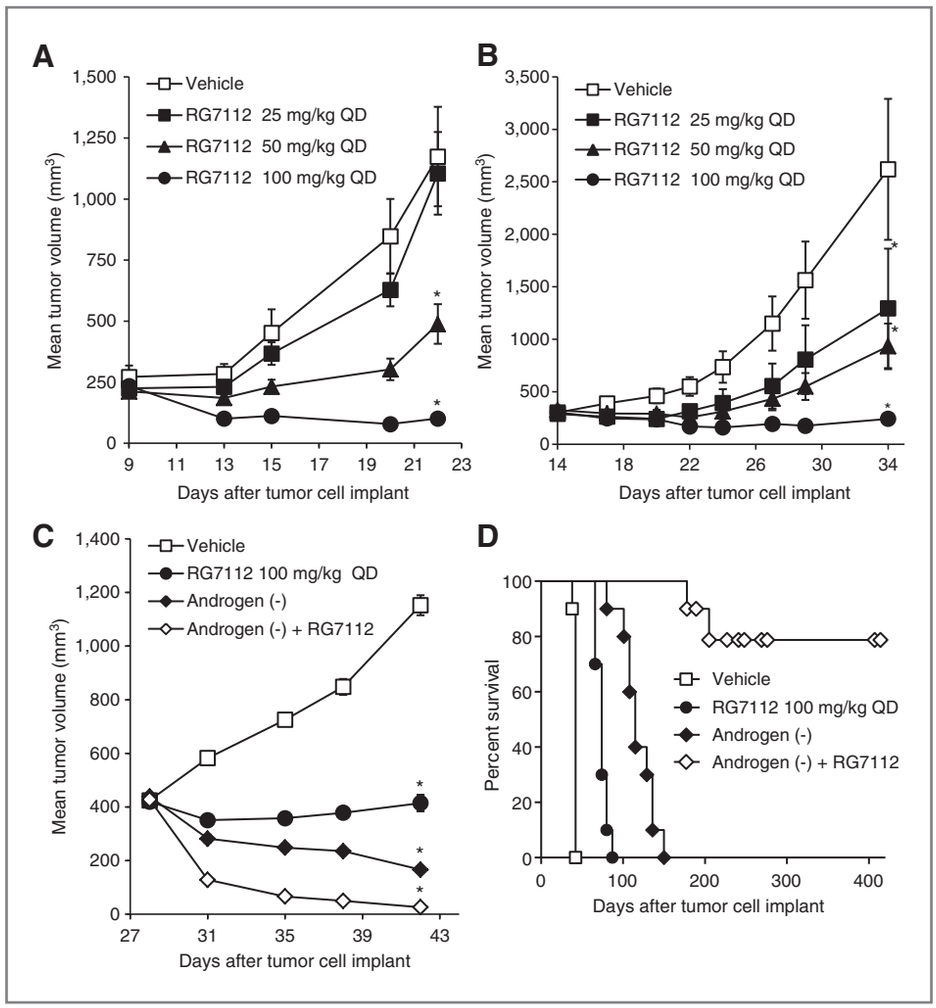

Figure 6. *In vivo* antitumor activity of RG7112. A–C, mice ($n = 10$/group) bearing established subcutaneous xenografts received vehicle or 25, 50, or 100 mg/kg of an oral suspension of RG7112 daily. Mice in androgen (-) groups had testosterone pellets removed. Tumor volumes were calipered throughout the study and data plotted as mean ± SEM. *, $P < 0.05$ versus vehicle control. A, SJSA-1; B, MHMn; C, LNCaP. D, LNCaP postcessation of treatment, mice were monitored for tumor regrowth and ILS was calculated by Kaplan–Meier using an endpoint of 1,000 mm^3 tumor volume. QD, once daily dose.

pronounced tumor regression with practically no palpable tumors left at the end of the 2-week treatment period (Fig. 6C). Kaplan–Meier survival analysis showed that each monotherapy substantially increased mouse lifespan (76% for RG7112; 174% for androgen withdrawal; Fig. 6D). However, the increase of lifespan (ILS) by the combination was more than 800%, indicating that most mice died from natural causes.

Discussion

The data reported here show that RG7112 is a potent and selective antagonist of the p53–MDM2 interaction that effectively activates the p53 pathway and induces cell-cycle arrest and/or apoptosis in cell lines expressing wild-type p53 and representing a variety of solid tumor types. In cell-free assays, RG7112 binds to MDM2 protein with high affinity ($K_D \sim 11$ nmol/L) and inhibits MDM2-p53 binding with $IC_{50} \sim 20$ nmol/L. Exposure of cultured cancer cells to the compound leads to a dose-dependent accumulation of p53 protein and activation of its transcriptional targets and the p53 pathway. As a result, cancer cells undergo a cell-cycle block in G_1 and G_2 phase followed by apoptosis.

RG7112 was most effective in killing cancer cells overproducing MDM2 protein as a result of *MDM2* gene amplification (e.g., SJSA1 and MHM osteosarcoma; Fig. 3B and C). However, despite its substantially increased potency, RG7112 was unable to induce effective cell death in more than half of the 12 solid tumor cell panels (Fig. 3C). As previously shown for nutlin-3a (16), this was not due to inability to stabilize p53 and activate its transcriptional targets and cell-cycle arrest function but likely to defective downstream p53 apoptotic signaling. The high sensitivity of MDM2-amplified tumors is likely due to the fact that these tumors are free of other defects in the p53 pathway and inhibition of MDM2 restores their full p53-dependent apoptotic potential.

Inhibition of cell-cycle progression is a major function of activated p53 and usually precedes induction of apoptosis (16, 22). Our data suggest that the cell-cycle in MDM2-amplified SJSA1 osteosarcoma cells can be blocked at lower RG7112 levels. The EC_{50} for cell-cycle arrest was 2.5-fold lower than EC_{50} for apoptosis (Fig. 3D). This difference in threshold levels may favor cell-cycle arrest over apoptosis. This is expected because cell-cycle arrest is one of the primary functions of p53 evolved to protect cells from propagation of damaged DNA

Published OnlineFirst February 11, 2013; DOI: 10.1158/0008-5472.CAN-12-2807

before it is repaired, whereas apoptosis is thought as the ultimate step for elimination of cells with unrepairable damage. We have shown previously that cell-cycle arrest by nongenotoxic p53 activation in SJSA1 and other cancer cell lines does not affect the ability of cancer cells to undergo apoptosis (17). The lower drug threshold for cell-cycle arrest may allow for partially separating the 2 effects of activated p53 in the clinical setting.

Another, interesting finding of this study is the independence of the onset of cell death on caspase activity (Fig. 4). Although caspase inhibition shifted the morphology of dying cells from typical apoptotic to a necrotic-like, it did not change the magnitude and kinetics of cell death. The ability of RG7112 to induce "caspase-independent" cell death suggests that alterations in caspase expression and activity, frequently found in human cancer, may not affect the overall outcome of MDM2 antagonist therapy as long as p53 downstream signaling in tumor cells is preserved.

Given orally to nude mice, RG7112 was able to penetrate human xenografts, effectively inhibited their proliferation, and induced apoptosis in a dose-dependent manner. As observed *in vitro*, cell-cycle arrest indicated by inhibition of BrdUrd incorporation preceded apoptosis induction, detected by both PARP1 cleavage and caspase-3/7 activation (Fig. 5). Daily administration of RG7112 to SJSA1 bearing nude mice for 3 weeks resulted in a dose-dependent suppression of tumor growth and regression in the high-dose group (100 mg/kg/day). Similar efficacy was observed in the MHM osteosarcoma model (Fig. 6) also expressing high levels of MDM2 protein (15). These results confirmed the *in vitro* observations that MDM2-amplified tumors are highly sensitive to MDM2 antagonists, which remove the major barrier to p53 functionality acquired during cancer development. Therefore, MDM2-amplified status of patients with wild-type p53 tumors could be a useful predictor of response to p53-activating therapy by MDM2 antagonists.

The high-genetic plasticity characteristic for human tumors, especially at advanced stages, increases the chances for acquired resistance to most single agent therapies including MDM2 antagonists. Therefore, combination approaches to cancer therapy are extensively sought. The p53 pathway is central to cancer cell signaling, interacting with multiple cellular pathways and offering opportunities for synthetic lethal strategies. The highly synergistic combination of p53 activation by RG7112 and androgen deprivation in the androgen-dependent LNCaP mouse model (Fig. 6C and D) is one example of these possibilities. Combination of RG7112 with androgen withdrawal, the standard for first-line prostate cancer therapy, led to a dramatic reduction of relatively large xenografts to unpalpable tumors and practically cured most mice.

The results presented in this article supported further evaluation of RG7112 in the clinic. Recently completed clinical biomarker studies in patients with liposarcoma have confirmed the ability of RG7112 to activate p53 and its major functions, cell-cycle arrest and apoptosis, in human tumors (23). Upcoming data from several ongoing clinical investigations should help to answer the question whether nongenotoxic p53 activation by MDM2 antagonists can improve the clinical outcomes for patients retaining wild-type p53 in their tumors.

Disclosure of Potential Conflicts of Interest

No potential conflicts of interest were disclosed.

Authors' Contributions

Conception and design: B. Graves, K. Packman, M. Linn, B. Vu, L. T. Vassilev
Development of methodology: K. Packman, R. Garrido, E. Lee, M. Linn
Acquisition of data (provided animals, acquired and managed patients, provided facilities, etc.): B. Graves, Z. Filipovic, M. Xia, C. Tardell, R. Garrido, K.-H. To, F. Podlaski, P. Wovkulich
Analysis and interpretation of data (e.g., statistical analysis, biostatistics, computational analysis): B. Graves, K. Packman, Z. Filipovic, M. Xia, R. Garrido, E. Lee, K.-H. To, M. Linn, F. Podlaski, L. T. Vassilev
Writing, review, and/or revision of the manuscript: B. Graves, K. Packman, R. Garrido, E. Lee, B. Vu, L. T. Vassilev
Administrative, technical, or material support (i.e., reporting or organizing data, constructing databases): B. Graves, Z. Filipovic, P. Wovkulich
Study supervision: B. Graves, L.T. Vassilev

Acknowledgments

The authors thank Karen Rowan, Ursula Kammlott, Christine Lukacs, Violeta Adames, Shahid Tannu, and Thelma Thompson for their experimental help and Kuo-Sen Huang, Nader Fotouhi, Steven Middleton, and David Heimbrook for stimulating discussions during the course of this study.

The costs of publication of this article were defrayed in part by the payment of page charges. This article must therefore be hereby marked *advertisement* in accordance with 18 U.S.C. Section 1734 solely to indicate this fact.

Received July 17, 2012; revised November 29, 2012; accepted December 17, 2012; published OnlineFirst February 11, 2013.

References

1. Vogelstein B, Lane D, Levine AJ. Surfing the p53 network. Nature 2000;408:307–10.
2. Harris SL, Levine AJ. The p53 pathway: positive and negative feedback loops. Oncogene 2005;24:2899–908.
3. Freedman DA, Wu L, Levine AJ. Functions of the MDM2 oncoprotein. Cell Mol Life Sci 1999;55:96–107.
4. Bond GL, Hu W, Levine AJ. MDM2 is a central node in the p53 pathway: 12 years and counting. Curr Cancer Drug Targets 2005;5:3–8.
5. Momand J, Zambetti GP, Olson DC, George D, Levine AJ. The mdm-2 oncogene product forms a complex with the p53 protein and inhibits p53-mediated transactivation. Cell 1992;69:1237–45.
6. Kubbutat MH, Jones SN, Vousden KH. Regulation of p53 stability by Mdm2. Nature 1997;387:299–303.
7. Marine JC, Lozano G. Mdm2-mediated ubiquitylation: p53 and beyond. Cell Death Differ 2010;17:93–102.
8. Picksley SM, Lane DP. The p53-mdm2 autoregulatory feedback loop: a paradigm for the regulation of growth control by p53? Bioessays 1993;15:689–90.
9. Michael D, Oren M. The p53-Mdm2 module and the ubiquitin system. Semin Cancer Biol 2003;13:49–58.
10. Vousden KH, Prives C. P53 and prognosis: new insights and further complexity. Cell 2005;120:7–10.
11. Vousden KH, Lu X. Live or let die: the cell's response to p53. Nat Rev Cancer 2002;2:594–604.
12. Poyurovsky MV, Prives C. Unleashing the power of p53: lessons from mice and men. Genes Dev 2006;20:125–31.

Published OnlineFirst February 11, 2013; DOI: 10.1158/0008-5472.CAN-12-2807

13. Brown CJ, Lain S, Verma CS, Fersht AR, Lane DP. Awakening guardian angels: drugging the p53 pathway. Nat Rev Cancer 2009;9:862–73.
14. Kussie PH, Gorina S, Marechal V, Elenbaas B, Moreau J, Levine AJ, et al. Structure of the MDM2 oncoprotein bound to the p53 tumor suppressor transactivation domain. Science 1996;274: 948–53.
15. Vassilev LT, Vu BT, Graves B, Carvajal D, Podlaski F, Filipovic Z, et al. *In vivo* activation of the p53 pathway by small-molecule antagonists of MDM2. Science 2004;303:844–8.
16. Tovar C, Rosinski J, Filipovic Z, Higgins B, Kolinsky K, Hilton H, et al. Small-molecule MDM2 antagonists reveal aberrant p53 signaling in cancer: implications for therapy. Proc Natl Acad Sci U S A 2006; 103:1888–93.
17. Tovar C, Higgins B, Kolinsky K, Xia M, Packman K, Heimbrook DC, et al. MDM2 antagonists boost antitumor effect of androgen withdrawal: implications for therapy of prostate cancer. Mol Cancer 2011; 10:49.
18. Yang H, Filipovic Z, Brown D, Breit SN, Vassilev LT. Macrophage inhibitory cytokine-1: a novel biomarker for p53 pathway activation. Mol Cancer Ther 2003;2:1023–9.
19. el-Deiry WS, Tokino T, Velculescu VE, Levy DB, Parsons R, Trent JM, et al. WAF1, a potential mediator of p53 tumor suppression. Cell 1993;75:817–25.
20. Harper JW, Adami GR, Wei N, Keyomarsi K, Elledge SJ. The p21 Cdk-interacting protein Cip1 is a potent inhibitor of G_1 cyclin-dependent kinases. Cell 1993;75:805–16.
21. Thompson T, Tovar C, Yang H, Carvajal D, Vu BT, Xu Q, et al. Phosphorylation of p53 on key serines is dispensable for transcriptional activation and apoptosis. J Biol Chem 2004;279:53015–22.
22. Vassilev LT. MDM2 inhibitors for cancer therapy. Trends Mol Med 2007;13:23–31.
23. Ray-Coquard I, Blay JY, Italiano A, Le Cesne A, Penel N, Zhi J, et al. Effect of the MDM2 antagonist RG7112 on the P53 pathway in patients with MDM2-amplified, well-differentiated or dedifferentiated liposarcoma: an exploratory proof-of-mechanism study. Lancet Oncol 2012;13:1133–40.

Published OnlineFirst February 11, 2013; DOI: 10.1158/0008-5472.CAN-12-2807

Cancer Research
The Journal of Cancer Research (1916–1930) | The American Journal of Cancer (1931–1940)

AACR American Association for Cancer Research

MDM2 Small-Molecule Antagonist RG7112 Activates p53 Signaling and Regresses Human Tumors in Preclinical Cancer Models

Christian Tovar, Bradford Graves, Kathryn Packman, et al.

Cancer Res 2013;73:2587-2597. Published OnlineFirst February 11, 2013.